Topics in Catalysis (2019) 62:117–128
https://doi.org/10.1007/s11244-018-1108-x

ORIGINAL PAPER

Mechanistic Aspect of N_2O Formation Over Pt–Ba/γ-Al_2O_3 Catalysts

I. S. Pieta[1] · M. Cortes-Reyes[2] · M. A. Larrubia[2] · L. J. Alemany[2] · W. S. Epling[3]

Published online: 12 December 2018

Abstract
NO_X reduction in lean-burn gasoline or diesel engines is challenging in the oxidizing environment, and depending on the after-treatment technology, can lead to by-product, such as N_2O or ammonia, formation. The current study focuses on possible N_2O formation pathways over NO_x storage/reduction (NSR) catalysts. More specifically, NH_3 reactivity with catalyst surface species was investigated over a model Pt–Ba/γ-Al_2O_3 (1/20/100, w/w) NSR catalyst with and without NO_x species stored (nitrites and nitrates). The NH_3 originates from reduction of NO_x in the regeneration phase. With NH_3, two overall reactions can lead to N_2 or N_2O formation, namely $3NO + 2NH_3 \rightarrow 5/2\ N_2 + 3H_2O$ and $4NO + NH_3 \rightarrow 5/2\ N_2O + 3/2H_2O$. These two are considered for catalyzed reaction between the entering NO and NH_3. Surface nitrite and nitrate reduction reactions leading to N_2 or N_2O were also evaluated, all as a function of temperature and relative amount of NH_3 in the gas phase. N_2O was formed in the lower temperature range, and was more significant with lower NH_3 concentrations. At higher temperatures, above 423 K, for NH_3 concentrations higher than stoichiometric, only N_2 was produced. In comparing the results from the samples with preformed nitrites/nitrates on the surface to those without, it is apparent that NH_3 first reacts with gas-phase NO and then with pre-stored surface NO_x species. Moreover, the reduction of surface nitrites/nitrates is complete only for high NH_3/NO ratios, and when NH_3 is the limiting reactant, they remain on the catalyst surface unreacted until temperatures higher than 623 K, where they decompose. In general, for all performed experiments, N_2O was the dominant product at low temperature, when NO and NH_3 conversions are low. At higher temperature, with increasing NO and NH_3 conversions, N_2 selectivity increases.

Keywords N_2O formation · Pt–Ba/Al_2O_3 · Catalyst regeneration · NO_x storage/reduction · Lean NO_x trap · Emissions reduction · Temperature programmed surface reaction · Operando DRIFTS

1 Introduction

Over the last few decades, stricter regulations on nitrogen oxide (NO_x) emissions have been implemented, to mitigate its impact on human health and the environment [1–4]. There are two technologies that have emerged as solutions for NO_x reduction, NO_x storage and reduction (NSR) catalysis and selective catalytic reduction (SCR) catalysis, as well as combining the two [5–7]. For SCR, the ammonia reactant is derived from hydrolysis of aqueous urea [8, 9]. Thus an extra tank of aqueous urea is needed and solutions that avoid this extra feature are desired. NSR is challenged by cost and sulfur poisoning, but avoids the need for an external reductant. The focus of this study is the NSR catalyst.

NSR technology works via a cyclic process, alternating between an oxidizing phase, called the lean phase, where the NO_x is stored as nitrites or nitrates, and a rich phase with a higher content of reducing compounds relative to oxygen, where the adsorbed NO_x species are reduced with ideally the formation of water and nitrogen [10, 11]. Model catalysts consist of a support with high surface area, such as alumina, a noble metal for the redox aspects and a storage element, which usually is an alkaline or alkaline-earth, such as barium [12, 13]. In addition, there has been research focused on

Electronic supplementary material The online version of this article (https://doi.org/10.1007/s11244-018-1108-x) contains supplementary material, which is available to authorized users.

✉ I. S. Pieta
ipieta@ichf.edu.pl

[1] Institute of Physical Chemistry PAS, Kasprzaka 44/52, 01-224 Warsaw, Poland

[2] Department of Engineering Chemistry, University of Malaga, 29071 Malaga, Spain

[3] Department of Chemical Engineering, University of Virginia, 102 Engineers' Way, Charlottesville, VA 22904-4741, USA

the modification of the model catalyst by the incorporation of other metals, e.g. potassium to improve the soot resistance, Sn to improve sulfur resistance or ceria to increase the NO_x adsorption and modify ammonia production [14–16]; or even the using other less expensive materials, such as perovskites [17]. Most of them have compared the catalysts in terms of oxidation and adsorption capacities but not so many papers have been focused on the reduction step of the cycle. Nitrogen selectivity is required, however, in certain conditions or depending on the materials, NH_3 and/or N_2O are observed, both undesired products that should not be emitted [18–21].

There have been several studies focused on understanding the role of different reductants that are present in the exhaust [22–24]. Some authors have compared the use of H_2 and C_3H_6 and have observed a HC-intermediate NO_x reduction pathway in addition to the well-stablished classical H_2-driven NSR pathway, but with a weaker contribution. The better low temperature performance with hydrogen is due to the Pt site poisoning by CO or hydrocarbons. However, at higher temperatures, regeneration performance becomes comparable between the three, and for hydrocarbons, steam reforming may contribute [25].

Ammonia can form via NO_x reduction during the regeneration phase, and this is the basis for the coupling of the NSR–SCR technologies [26–28]. It is noteworthy that parallel undesired reactions can also occur. The formation of N_2O has been analyzed under different operation conditions, shown to be dependent on cycle frequency and temperature, when H_2 or CO are used as the reductant [29]. In general, N_2O production during the regeneration phase is not as significant when the reductants are highly active, i.e. at higher temperature for example, leading to high N_2 selectivity [30]. For example, H_2 leads to more N_2O at lower temperatures, 200 °C, but propylene at 300 °C, where its activation begins [31]. In addition, the use of C_3H_6 as a reducing agent involves a reaction network that includes NCO species, that leads to N_2O during the lean phase, but this is reduced in the presence of water [32]. When CO or C_3H_6 are fed, N_2O production is higher relative to H_2 being used, due to the formation of isocyanates and CO adsorbed on Pt sites [33].

Although there has been recent research, with some highlights mentioned above, focused on N_2O formation, the relationship between the ammonia formed and reduction of the nitrate or nitrite species, or reaction with exhaust NO, leading to N_2O formation has not been resolved. Therefore, in this paper we report a study focused on N_2O formation during the regeneration step over a model Pt–Ba/Al_2O_3 catalyst using by-product NH_3 as the reductant. Moreover, the study quantifies ammonia consumption, taking into account the presence of NO, and the reacted ammonia selectivity toward N_2 as well as toward undesired N_2O, under different stoichiometric conditions.

2 Materials and Methods

2.1 Catalyst Preparation and Characterization

The Pt–Ba/γ-Al_2O_3 (1/20/100, w/w) catalyst was prepared by a two-step process. First, the Pt/γ-Al_2O_3 sample was made with a first impregnation of γ-Al_2O_3 (Puralox, Sasol, surface area 200 m^3/g, pore volume 0.7 m^3/g) using a solution of $Pt(NH_3)_2(NO_2)_2$ (diamminedinitroplatinum (II) ($Pt(NH_3)_2(NO_2)_2$), Pt content 3.4 wt%, density 1.05 g ml^{-1}, Aldrich Chemical) followed by drying at 373 K and calcination at 773 K for 5 h. Ba was added to this Pt/Al_2O_3 via incipient wetness using an aqueous solution of $Ba(CH_3COO)_2$ (Merck, 99%). The final calcination was carried out at 773 K, in air for 5 h. More detailed information about the catalyst preparation and properties were given previously [20, 34].

2.2 Activity Study

The reaction studies were performed in a quartz fixed-bed reactor connected to a QMS 200 mass spectrometer (Pfeiffer Vacuum Prisma™) for outlet gas analysis and the sample temperature was measured by a thermocouple placed directly into the catalyst bed. 60 mg (100–120 μm) of the catalyst sample was used in each test with a constant total flow of 100 ml min^{-1}. The mass spectrometer (MS) was well-calibrated, eliminating the cross sensitivity effect of the species presented in the gas mixture, to allow NO, N_2O and NO_2 measurements. The following mass-to-charge ratios were used to monitor the evolution of reactant/product concentration profiles during reaction: 2 (H_2), 15 (NH_3), 18 (H_2O), 28 (N_2), 30 ($NO_x = NO + NO_2$), 32 (O_2), 40 (Ar), 44 (N_2O), 46 (NO_2). For additional information, supplementary mass-to-charge ratios were taken into account: 12 (secondary ionization of CO_2), 14 (secondary ionization of N_2), 16 (100% signal of NH_3). The interferences of the mass-to-charge ratios were considered during data analysis and MS signal to concentration (ppm) calculations. The MS data were quantitatively analyzed using factors determined experimentally during the calibration process. For calibration, calibration mixtures were used and fragmentation patterns were recorded.

Prior to an experiment, a temperature programmed desorption (TPD) in He was done to provide a clean catalyst surface. The TPD conditions were 300–773 K, 10 K min^{-1}. Temperature-programmed surface reactions (TPSR) were performed in feed streams containing NO (NO-TPSR), NH_3

(NH_3-TPSR) and NO + NH_3 (NO + NH_3-TPSR), with He as the balance gas.

For NO-TPSR, 500 ppm of NO was used for catalyst exposure to saturation and the 500 ppm NO concentration was maintained during the TPD, which was from room temperature to 773 K with a ramp of 10 K min^{-1}. Similarly, for the NH_3-TPSR experiments, the sample was exposed to 333 ppm of NH_3 to saturation and then followed by the TPD with NH_3 still present in the gas phase.

The TPSR experiments were carried out over a catalyst without preformed nitrites/nitrates (experiment type I) and for a catalyst with preformed nitrites/nitrates on the surface (experiment type II). For both types NO + NH_3-TPSR type I and II, three ammonia concentrations were used, 166, 333 and 1000 ppm NH_3, while keeping the NO at 500 ppm. For all experiments, first NO was admitted to the reactor at RT and after NO saturation, ammonia was added to the flow until ammonia saturation. The sample was then heated up to 723 K with a ramp of 10 K min^{-1}. This admittedly leads to formation of surface NO_x species, specifically nitrites as will be discussed below. However, the amounts are significantly less than those found in the type II experiments.

In the case of TPSR with preformed nitrites/nitrates, type II, prior to TPSR nitrites/nitrates were formed over the catalyst samples. The nitrites/nitrates storage were performed during lean-rich cycling applying transient response method (TRM) at 623 K (GHSV = 1.5×10^5 h^{-1}, at 1 atm and 293 K). A rectangular pulse of NO (1000 ppm) + O_2 (3%) in He flow and H_2 (2000 ppm) in He flow were subsequently fed during the oxidation and reduction steps, respectively. There was no He purge applied between the lean and rich stepswas admitted to the reactor. After 4–5 adsorption–reduction cycles at given temperature, a stable catalyst behavior was obtained and nitrites–nitrates storage has been performed. The amounts of stored nitrites/nitrates were estimated taking into account that the amount of stored nitrites/nitrates is proportional to the area A1 in Fig. S1.

After the storage step, the catalyst was cooled in He to RT and the NO + NH_3-TPSR was performed. To ensure the complete removal of the stored nitrites/nitrates, a regeneration phase included exposure to 1000 ppm of NH_3 in He at 623 K at the end of TPSR type II, followed by the TPD up to 723K. The calculated selectivities to N_2 (S_{N_2}) and to N_2O (S_{N_2O}) are based on molar amounts of N_2, N_2O, NO and NO_2 produced. The calculated Nbalance closed with an error less than 57%.

Diffuse reflectance infrared Fourier transform spectroscopy (DRIFTS) studies were performed in a continuous flow Harrick Praying Mantis reaction chamber. A FTIR Nicolet Nexus 470 spectrometer was used to characterize the interactions between the gas species and the catalyst surface during the TPSR experiments. The reactions were carried out in a temperature range between room temperature and 723 K. Spectra were recorded in diffuse reflectance mode, and 45 scans were collected at a resolution of 1 cm^{-1} (Table 1).

3 Results and Discussion

3.1 NH_3 versus H_2 Reduction of Nitrites/Nitrates

Figure 1 shows the reduction of nitrites/nitrates stored over Pt–Ba/Al_2O_3 using H_2 (Fig. 1a) and NH_3 (Fig. 1b, c). Upon H_2 admission to the reactor at t = 0 s, H_2 was completely consumed for about 180 s and then, the H_2 outlet concentration gradually increased with time, reaching the inlet value at ca. 1400s. N_2 was formed and after 350 s, NH_3 was observed, reaching ca. 100 ppm. H_2O was also observed as a product, reaching 1300 ppm after 200 s. The amounts of N_2 and H_2O produced is close to the 1:5 ratio, indicating nitrites/nitrates reduction through reactions (1) and (2). In line with literature no N_2O was observed under these conditions [18, 20, 49, 50].

$$3Ba(NO_3)_2 + 5H_2 \rightarrow N_2 + 5H_2O + BaO \quad (1)$$

$$3Ba(NO_3)_2 + 8H_2 \rightarrow 2NH_3 + 5H_2O + BaO \quad (2)$$

The results obtained during the reduction of stored NO_x with different amounts of NH_3, 1500 versus 2500 ppm, are presented in Fig. 1b, c. In the experiment with 1500 ppm NH_3, Fig. 1c, full reductant consumption and N_2 production occurred for ca. 85 and 250 s, respectively. Increasing the NH_3 concentration led to faster regeneration, Fig. 1b. The NH_3 consumption and N_2 production time decrease by ca. 50% in comparison to the same experiment with less NH_3, although less than twice as much was added. With 2000 ppm NH_3, the regeneration time decreased by ca. 70% compared to H_2, although on a per H basis it should have been only 50% if linearly correlated to reductant amount. These results indicate that for the given reaction conditions, at 623 K NH_3 is a more efficient reducing agent than H_2 (Fig. 1d).

Based on the results obtained during these specific experiments, reaction (3) is sufficient to explain the reaction stoichiometry, with the error ($N_{adsorbed}/N_{produced}$) found to be in the 3–5% range.

$$3Ba(NO_3)_2 + 10NH_3 \rightarrow 8N_2 + 15H_2O + 3BaO \quad (3)$$

The obtained data reveal that under similar conditions, the reduction of stored NO_x was much faster with NH_3 compared to H_2. All these results also show high reactivity between NO and H_2. With increasing NH_3 concentration, the reaction onset temperature was not significantly changed, and with H_2 as a reductant NH_3 formation was detected among the reaction products, what is in line with previous study [51]. Ultimately, N_2 is formed, and possible pathways for its production have been proposed, involving

Table 1 Assignments of peak positions in DRIFT spectra results

Wavenumber [cm^{-1}]	Assignment	References
1650–1610	Bridging bidentate nitrate, ν(N=O)	[35–37]
1260–1210	Bridging bidentate nitrate, $\nu(NO_{2as})$	
1590–1540	Chelating bidentate nitrate, ν(N=O)	[35–38]
1320–1290	Chelating bidentate nitrate, $\nu(NO_{2as})$	
1550	Monodentate nitrate, $\nu(NO_{2as})$	[37, 39]
1257	Monodentate nitrate, $\nu(NO_{2asym})$	
1480	Linear nitrate, ν(N=O)	[36–38, 40, 41]
1300	Bridging bidentate nitrite, $\nu(NO_{2as})$	[35–37]
1230	Bridging bidentate nitrite, $\nu(NO_{2sym})$	
1160	Bridged N-coordinated nitrite, ν(N=O)	[36]
2146	–C≡N, ν(C≡N)	[42]
2280–2230	–NCO on Al^{3+}, out-of-phase ν(N=C=O)	[35, 38, 41]
2160–2170	–NCO on Ba, out-of-phase ν(N=C=O)	[35, 36, 39, 43–45]
Carbon base adsorbates [37, 41, 42, 45–48]		
1648, 1256 and 990	Bridged bidentate carbonate	
1599, 1310	Carboxylate ion	
1545, 1363	Chelating bidentate carbonate	
1408, 1091	Carbonate ion	
1975	Bridged CO	
2000–2080	Pt bound CO	
2347	Gas CO_2	

NO adsorption on reduced Pt particles, followed by decomposition to N and O ad-species [19, 51, 52].

$O_{(ads)}$ species are removed by H_2, leading to water formation. Along similar lines, the presence of NH_3, observed for high H_2 concentrations, would be due to reaction between N and H ad-species [51]. Ba also apparently plays a role in those reactions. It has been reported that Ba addition to supported Pt catalysts results in an increase in NO_x reduction activity in the absence of O_2 [19, 52, 53]. It was suggested that according to reactions (4)–(6), the presence of the alkaline or alkaline-earth metal ion weakens the N–O bond [54]. This will favor dissociation and subsequent reduction. The addition of Ba also increases the selectivity of the reaction to N_2.

In the case of ammonia as a reductant, previous studies have shown that it behaves similar to H_2, with the same NO_x conversion efficiency [55, 56]. On the other hand, some literature data have revealed a difference in NH_3 versus H_2 reactivity towards stored NO_x, for different catalyst compositions [50]. Specifically, a higher reactivity of ammonia for Pt–K/Al_2O_3 regeneration was noted relative to Pt–Ba/Al_2O_3, possibly due to the different nature of stored nitrites/nitrates (different ionic/bidentate ratio) and the Pt sites. In the results shown in Fig. 1, the reductant choice influenced the reduction rate. As the same catalyst was used for both experiments, it is not a difference in initial surface species type. In order to better understand the NH_3 reactivity with NSR catalyst surface species, TPSR experiments were carried out over the nitrite/nitrate-free (or at least minimized) Pt–Ba/Al_2O_3 and for the same catalyst with nitrites/nitrates on the surface.

3.2 TPSR over a Catalyst Without Preformed Nitrites/Nitrates

TPSR experiments over the sample without preformed nitrates/nitrites can help isolate the reaction between gas phase NO and NH_3. First, an NO-TPSR was examined (Fig. 2), and reveals N_2O formation with a maximum at 657 K, likely through NO decomposition on Pt. The *operando* DRIFTS study (Fig. S2) showed mostly nitrite formation on the surface, with two main peaks located at 1300 and 1230 cm^{-1}.

The NO + NH_3-TPSR results from the sample without preformed nitrates/nitrites are shown in Fig. 3, with corresponding in situ DRIFTS catalyst surface analysis shown in Fig. S3. The DRIFTS results show mainly nitrite formation on Ba sites, similar as in case with NO- and NH_3-TPSR (peaks at 1300 and 1230 cm^{-1}, Fig. S3 lines NN350 and NN He vs Fig. S2a and b). At the beginning of the (NO + NH_3)-TPSR reaction, all experiments show an ammonia desorption peak as the temperature increased (Fig. 3). With 500 ppm NO + 166 ppm

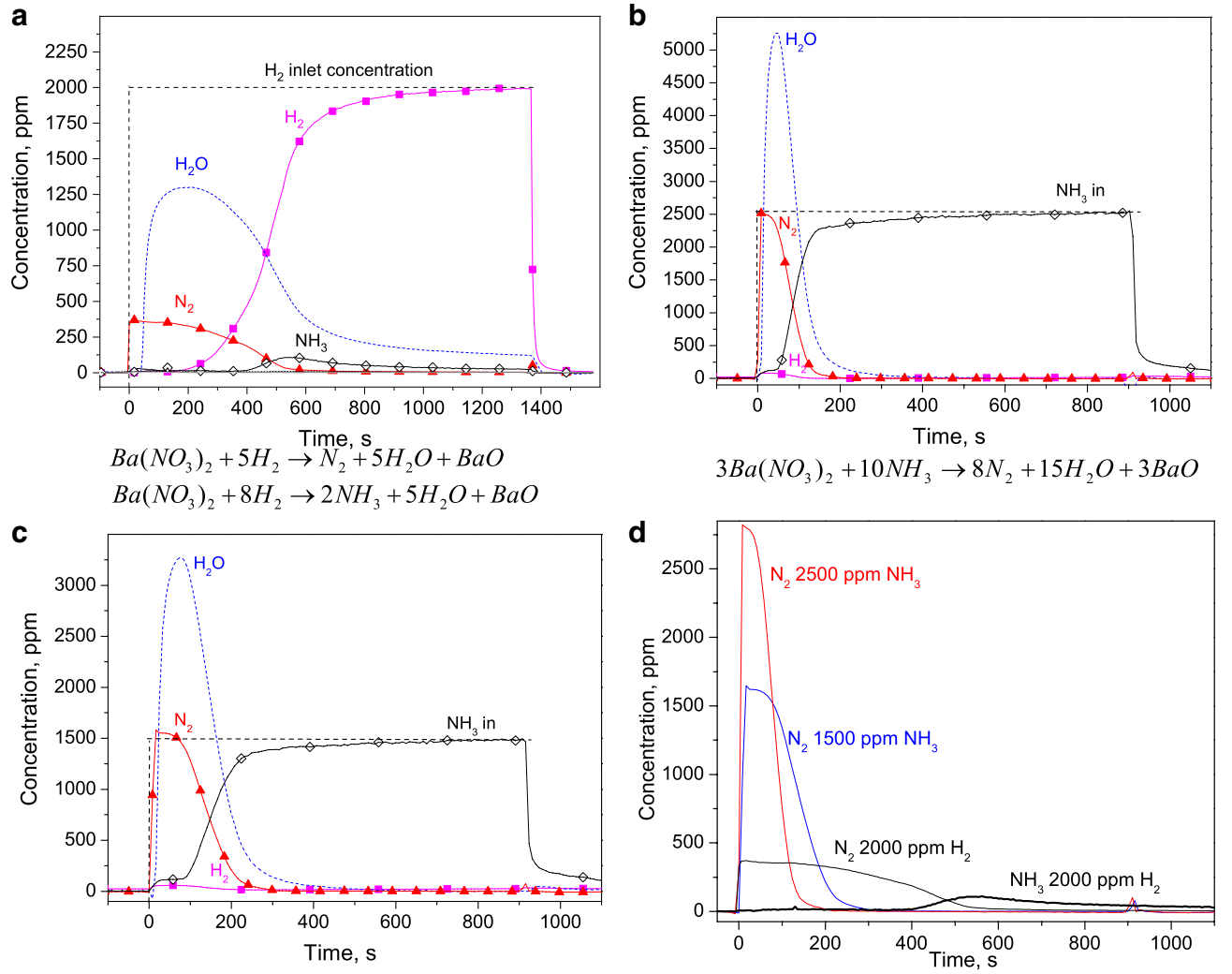

$$Ba(NO_3)_2 + 5H_2 \rightarrow N_2 + 5H_2O + BaO$$

$$Ba(NO_3)_2 + 8H_2 \rightarrow 2NH_3 + 5H_2O + BaO$$

$$3Ba(NO_3)_2 + 10NH_3 \rightarrow 8N_2 + 15H_2O + 3BaO$$

Fig. 1 TRM profile for the Pt–Ba/Al_{Pox} catalyst during rich phase **a** 2000 ppm of H_2 in He, **b** 1500 ppm, **c** 2500 ppm of NH_3 in He at 623 K, **d** H_2 vs NH_3 in He comparison. Total flow 100 ml min^{-1}

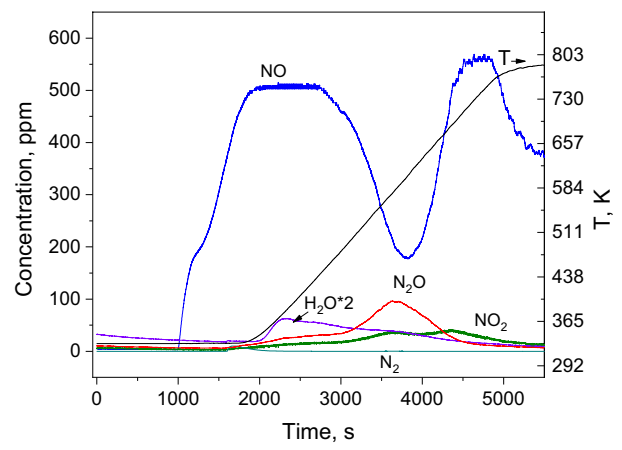

Fig. 2 NO-TPSR profile for the Pt–Ba/Al_{Pox} catalyst 500 ppm of NO in He. Total flow 100 ml min^{-1}

NH_3 (Fig. 3), the maximum NO consumption occurs between 423 and 473 K and more product N_2O, relative to N_2, was detected. The results for TPSR experiments with higher NH_3 concentration (333 and 1000 ppm, Fig. 3b, c) showed, that for these conditions, NO reduction by NH_3 over Pt–Ba/Al_2O_3 produces only N_2 (1.43 and 1.48 × 10^{-3} mol/g_{cat}) above 423 K. In the 323–423 K temperature range, N_2O is formed, however the overall amounts of N_2O produced are below ca. 5 × 10^{-5} mol/g_{cat}. The amounts of N_2O and N_2 detected most likely correspond to the following global reactions:

$$3NO + 2NH_3 \rightarrow {}^{5}/_{2}N_2 + 3H_2O \quad (4)$$

$$4NO + NH_3 \rightarrow {}^{5}/_{2}N_2O + {}^{3}/_{2}H_2O \quad (5)$$

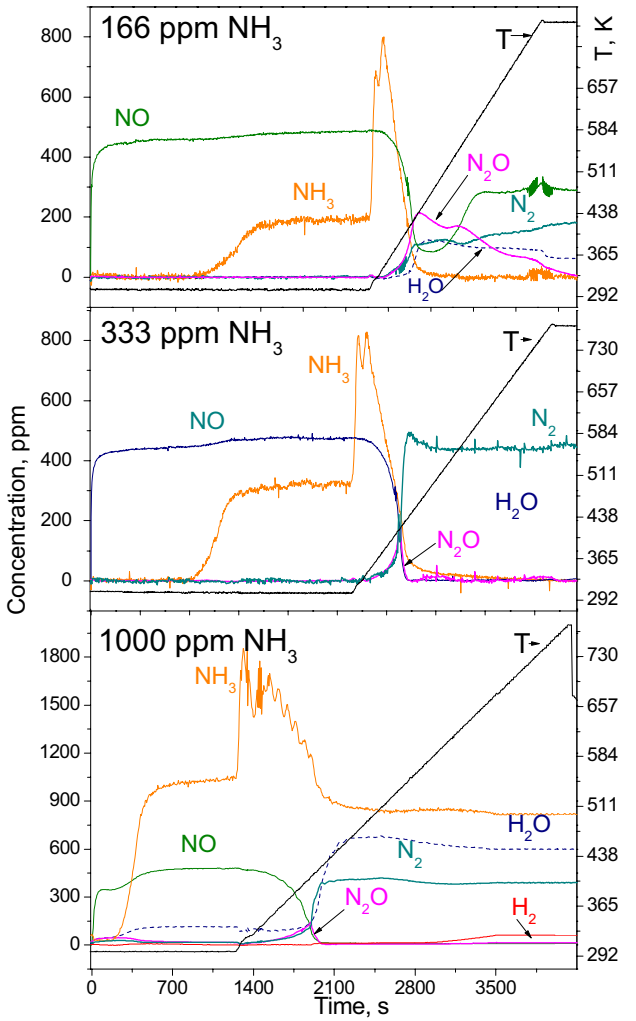

Fig. 3 Reactivity of 500 ppm NO and **a** 1000, **b** 333 and **c** 166 ppm of NH_3 over the Pt–Ba/Al_{Pox} catalyst without preformed nitrites/nitrates—TPSR type I. Flow 100 ml min^{-1}, He as a carrier. T ramp 10 K min^{-1}

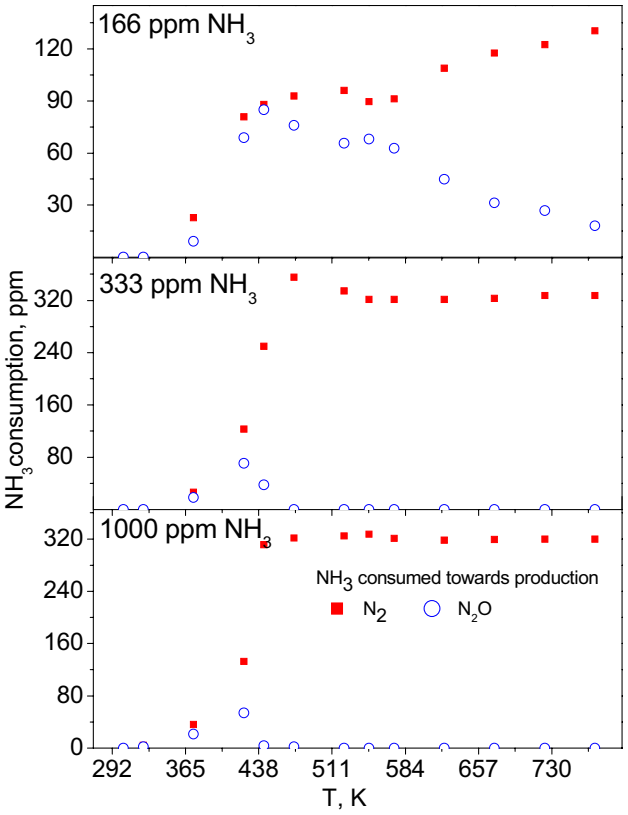

Fig. 4 Temperature dependence of reaction participation towards N_2 and N_2O over Pt–Ba/Al_{Pox} in the presence of: **a** 500 ppm NO + 1000 ppm NH_3, **b** 500 ppm NO + 333 ppm NH_3 and **c** 500 ppm NO + 166 ppm NH_3. Total flow 100 ml min^{-1}, He as a carrier

As was shown in Fig. 3, N_2O via reaction (5) dominates at low ammonia concentration (Fig. 3a) and conversion (up to 438 K Fig. 3a–c). The higher NO consumption at 423–473 K, compared to that at temperatures above 473 K, is probably due to the stoichiometry of reactions (4) and (5). However, the relative significance of the two reactions changes with temperature in such a way that at low temperatures reaction (5) dominates and at higher temperatures, its importance decreases. Also at higher temperatures, above ca. 573–623 K, N_2O can decompose [57]. For reaction (4), the opposite trends occur. It participates in the TPSR process more significantly above 473 K in all cases.

The mechanism N_2O formation describes the recombination of N-species on reduced Pt particles. Previous studies showed that the recombination of N ad-species gives N_2 as a product and recombination of N and NO ad-species leads to N_2O formation according to reactions (6)–(8) [54, 58, 59].

$$NO_{(g)} \rightarrow NO_{(ads)} \rightarrow N_{(ads)} + O_{(ads)} \quad (6)$$

$$N_{(ads)} + N_{(ads)} \rightarrow N_{2(g)} \quad (7)$$

$$NO_{(ads)} + N_{(ads)} \rightarrow N_2O_{(g)} \quad (8)$$

Moreover it was shown that the addition of Ba, especially its presence in close proximity to Pt, also increases the selectivity of the reaction to N_2. This enhanced selectivity was associated with the increase in the NO dissociation rate, which decreases the formation of N_2O according to reaction (8) [54].

In Fig. 4, the calculated amount of ammonia consumption towards N_2 and N_2O formation is shown for different NH_3 concentrations (166, 333 and 1000 ppm). For low ammonia concentration, reaction (5) plays an important role up to 773 K (Fig. 4, 166 ppm), while with higher ammonia concentrations (333 and 1000 ppm, Fig. 4), at temperatures above 473 K the contribution of reaction (5) to the total consumption of ammonia is negligible. For all TPSR type

I experiments, the maximum consumption of ammonia via reaction (5) occurs at ca. 423–448 K (Fig. 4) and at temperatures higher than 473 K an increase in the total amount of ammonia reacted toward N_2 production was observed. At the later stage of the TPSR reaction, above 473 K, the estimated NH_3 consumption values are roughly consistent with ammonia concentration inlets.

According to the results above, the amounts of N_2O produced depend on ammonia concentration and the reaction temperature. In Fig. 5, N_2O production during ($NO + NH_3$)-TPSR using 166, 333 and 1000 ppm of NH_3 is presented.

In general, N_2O is a dominant product at low temperature, when the NH_3 conversion is low. The largest amount of N_2O was produced during the experiment with 166 ppm of ammonia (Fig. 5a), around 3.81×10^{-4} mol/g_{cat}, and for this ammonia concentration most likely reaction (5) dominates till ca. 548 K. For higher ammonia concentrations (Fig. 5b, c), reaction (5) occurs in a narrow temperature window, ca. 323–373 K, and the values of N_2O produced decreased by ~90% with respect to the experiment with 166 ppm NH_3. Moreover, for higher ammonia concentrations, reaction (4) starts to dominate at much lower temperatures, at ca. 423 K. This may suggest that there is a minimum temperature, which limits reaction (4). This temperature would be tied to NH_3 activation on Pt sites or product desorption from the catalyst surface. Characterizing the slopes of the N_2O and N_2 concentration profiles, up to 323 K, leads to the assumption that the reaction rates for all experiments are similar. Moreover, the amounts of N_2O and N_2 produced up to 323 K indicate that the rates of reaction most likely are not controlled by ammonia concentration.

In general, during NO assisted TPSR experiment type I, with higher than stoichiometric ammonia concentrations, reaction (5) is practically negligible and N_2 is a dominant product through all experiments. At lower ammonia concentrations, more N_2O will form as shown in Fig. 5.

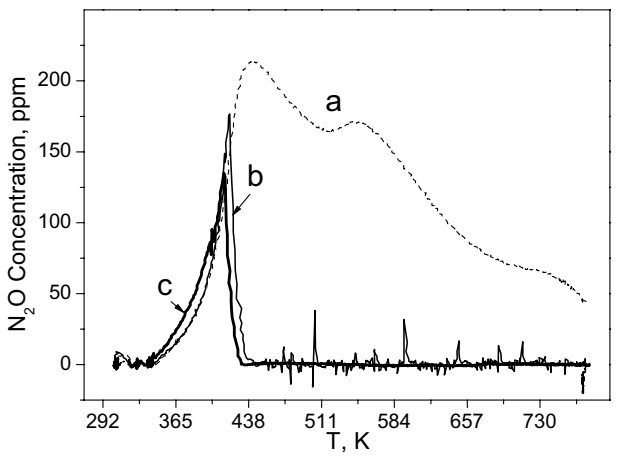

Fig. 5 N_2O production during TPSR type I experiment upon admission of 500 ppm of NO and **a** 166 ppm, **b** 333 ppm and **c** 1000 ppm of NH_3

3.3 TPSR over Catalyst with Preformed Nitrites/Nitrates

The TPSR type II experiments, with nitrites/nitrates preformed on the catalyst surface, were carried out in order to clarify the role of the NO-NH_3 reaction during the reduction of surface nitrates/nitrites (regeneration of the NSR catalyst) and also to compare the reactivity of NH_3 with the gas-phase NO entering the reactor, still of course on the catalyst surface, or the nitrite/nitrate species on the catalyst surface, or if both reactions take place together (Figs. 6, 7, 8, with corresponding in situ DRIFTs spectra shown in Fig. 9).

NO-TPSR data are shown in Fig. 6, where species evolution are plotted as a function of time along with temperature.

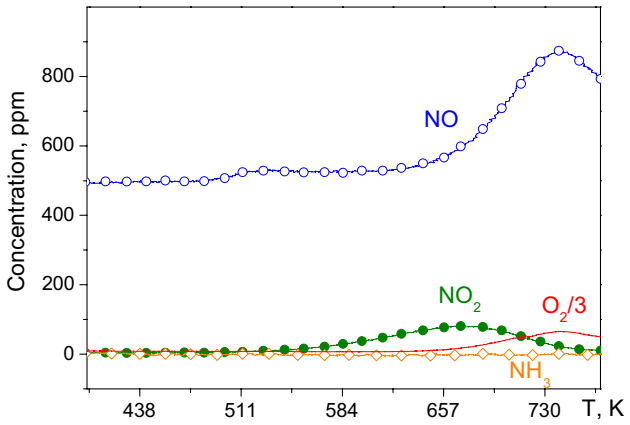

Fig. 6 NO-TPSR over Pt–Ba/Al_{Pox} catalyst with nitrites/nitrates preformed. Flow 100 ml min^{-1}, gas composition 500 ppm NO in He, Tramp 10 K min min^{-1}

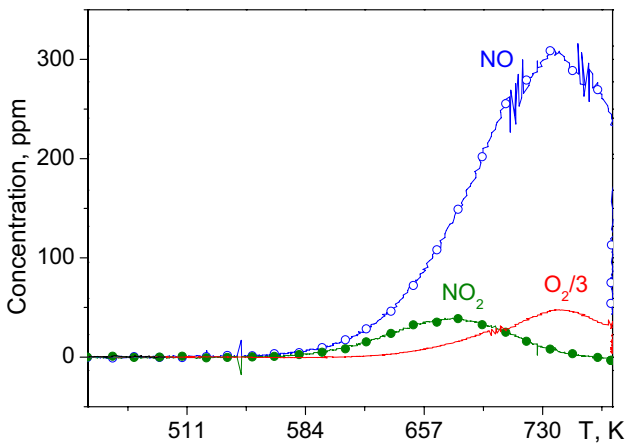

Fig. 7 He-TPD over Pt–Ba/Al_{Pox} catalyst with nitrites/nitrates preformed. Flow He 100 ml min^{-1}. Tramp 10 K min min^{-1}

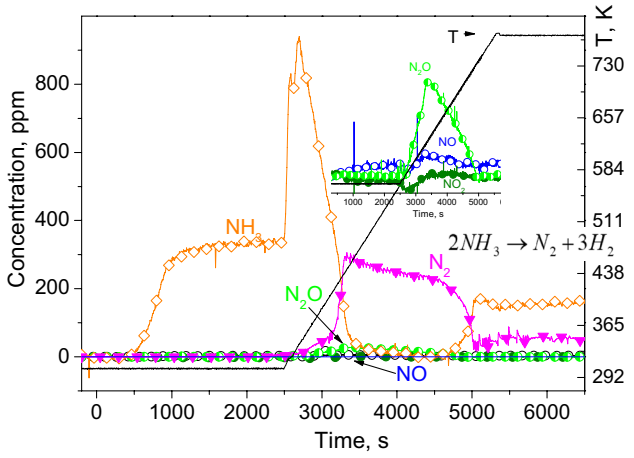

Fig. 8 NH_3-TPSR over Pt–Ba/Al_{Pox} catalyst with nitrites/nitrates preformed. Flow 100 ml min^{-1}, gas composition 333 ppm NH_3 in He, Tramp 10 K min^{-1}

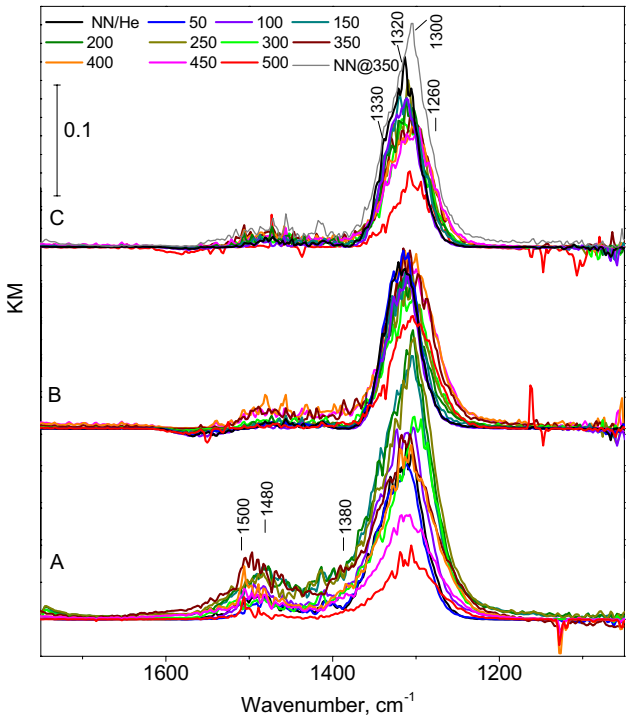

Fig. 9 In situ DRIFT spectra for Pt–Ba/Al_{Pox} catalyst with nitrites/nitrates preformed. Gas composition: **a** 333 of NH_3 in He, **b** 500 ppm NO in He, and **c** He. Flow 100 ml min^{-1}. T ramp 10 K min^{-1}

For this reaction, little influence of NO on the decomposition of the stored nitrites/nitrates was found (NO_x-species stored shown Fig. 9a–c lines NN350, NNHe). Apart from the higher NO concentration, the evolution of NO at temperatures higher than 623 K resembled those obtained for just nitrate decomposition in He (Fig. 7). However it is worth mentioning that nitrite/nitrate decomposition in the presence of He starts at ca. 50 K lower and slightly more NO_2 is produced when compared to nitrite/nitrate decomposition during NO-TPD. The maximum in nitrite/nitrate decomposition occurred at ca. 723 K. In both experiments (TPD in He and TPD in NO + He), after reaction ca. 6–9% of nitrite/nitrates remain on the catalyst surface as unreacted or stable; however they can be removed by a short H_2 or ammonia pulse at 723 K. The amounts of NO_x detected from nitrite/nitrate decomposition are consistent with the amounts of NO_x stored during the lean phase of the experiment and the mass balance error was found to be less than 8%.

During the NH_3-TPSR type II experiment with the Pt–Ba/Al_2O_3 catalyst, complete nitrite/nitrate reduction was achieved as shown in Fig. 8. The amounts of N_2O, NO and N_2 produced during the experiment correspond to the amounts of NO_x stored during the adsorption step. Reduction occurs from ca. 373 K up to ca. 673 K, however below 423 K the reduction of stored nitrite/nitrates is only partial. Based on these data, at this temperature the reaction probably is under kinetic control and the N-adsorbed species decomposition and/or reactivity of ammonia will limit the reaction. Above 443–473 K, reduction is fast and the reaction rate and product distribution are controlled by ammonia concentration. Moreover, for the NH_3TPSR experiment, decomposition of ammonia was detected at temperatures higher than 623 K and the amount of H_2 and N_2 (ratio 1:3), observed at the end of the NH_3-TPSR experiment, correspond to the stoichiometry of reaction (9).

$$2NH_3 \rightarrow N_2 + 3H_2 \quad (9)$$

N_2O production is small and the reaction is highly selective to N_2. The amount of the N_2O produced through all experiments was lower than that observed over the samples without preformed nitrites/nitrates with 500 ppm of NO and 333 ppm NH_3 (Fig. 8), and was below 5×10^{-5} mol/g_{cat}.

In situ DRIFTS spectra are shown in Fig. 9 for the experiment with nitrites/nitrates preformed; NH_3–TPSR (Fig. 9a), NO–TPSR (Fig. 9b) and nitrite/nitrate decomposition in He (Fig. 9c). The spectra recorded during NH_3–TPSR shows gradual consumption of nitrites (bands at 1300 and 1230 cm^{-1}) and a small amount of linear and bidentate nitrates (bands at 1480 and 1510 cm^{-1}) with increasing temperature. The formation of any other surface species was not evident during this experiment. At 773 K only a small amount of residual nitrite species are still present, 1300 cm^{-1}. Similar results were obtained for NO–TPSR (Fig. 9b) and nitrite/nitrate decomposition in He (Fig. 9c). For these experiments, the nitrites/nitrates decomposed also without other surface species formation. The highest amount of remaining nitrite species at 773 K occurred with the NO–TPSR experiment (Fig. 9b).

The results of the TPSR experiment with preformed nitrates/nitrites are shown in Fig. 10. For low ammonia

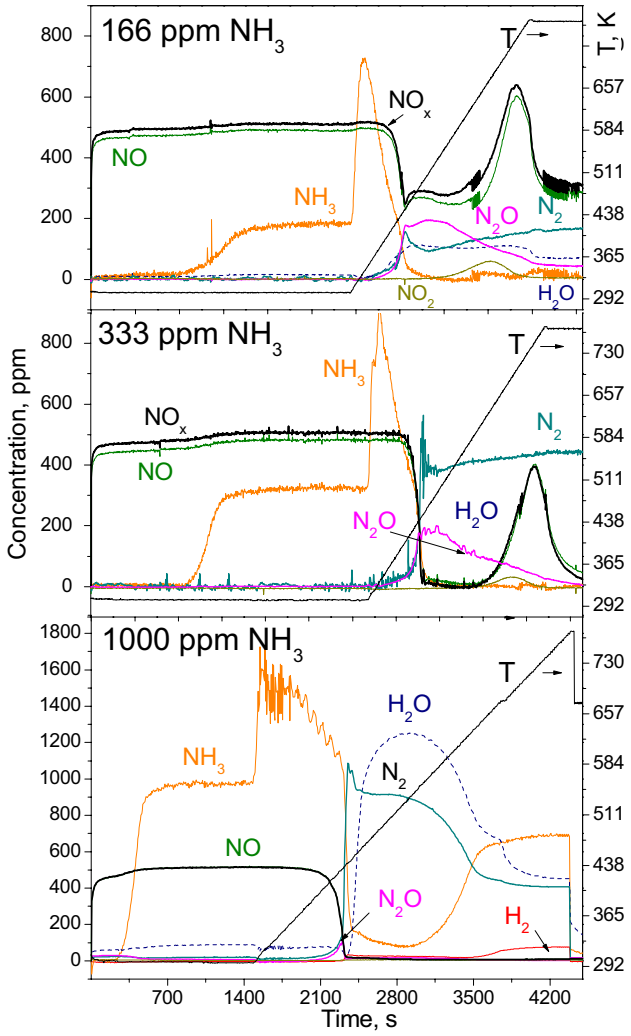

Fig. 10 Reactivity of 500 ppm NO and **a** 1000, **b** 333 and **c** 166 ppm of NH_3 over Pt–Ba/Al_{Pox} catalyst with nitrites/nitrates preformed—TPSR type II. Flow 100 ml min^{-1}, He as a carrier. Tramp 10 K min^{-1}

concentration (500 ppm NO + 166 ppm NH_3), the N_2O profile resembled that for (NO + NH_3)-TPSR over the catalyst with no preformed nitrites/nitrates (Fig. 3). At the beginning of the (NO + NH_3)-TPSR reaction, all experiments show an ammonia desorption peak as the temperature increased (Fig. 10 vs 3). With 500 ppm NO + 166 ppm NH_3 (Fig. 10), the maximum NO consumption occurs between 423 and 473 K with N_2O and N_2 formation. Nitrite/nitrate decomposition is observed between 657 and 773 K, similarly as in case of NO-TPSR with nitrites/nitrates preformed (Fig. 6). In this temperature range, the nitrites/nitrates decomposition for a stoichiometric NO:NH_3 ratio, i.e. 500 ppm NO + 333 ppm NH_3 is also observed. The results for TPSR experiments with higher NH_3 concentration (333 and 1000 ppm) showed, that for these conditions, NO reduction by NH_3 reacts to form only N_2 above 423 K. In the 323–423 K temperature range,

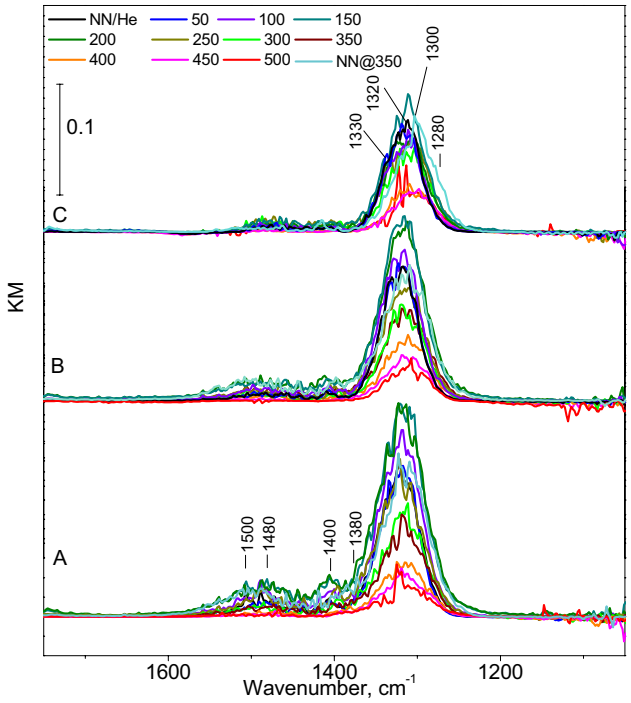

Fig. 11 In situ DRIFT spectra for a Pt–Ba/Al_{Pox} catalyst with nitrites/nitrates preformed—TPSR type II. Gas composition: 500 ppm NO and **a** 1000, **b** 333 and **c** 166 ppm of NH_3 in He. Flow 100 ml min^{-1}. T ramp 10 K min^{-1}

N_2O is formed. For the higher ammonia concentrations, NH_3 decomposition was evident. It can be assumed that reaction (5) dominates from the beginning of the reaction test up to ca. 623 K. Above this temperature the NO peak reaches its maximum at 723 K. This peak can be attributed to nitrate/nitrite decomposition as they become unstable, similar as what was observed for NO-TPSR, Fig. 6.

The in situ DRIFTS spectra obtained during (NO + NH_3)-TPSR with nitrites/nitrates preformed are shown in Fig. 11. The spectra resemble those obtained during NH_3–TPSR (Fig. 9a). Upon NH_3 admission, there is gradual consumption of nitrites (bands at 1300 and 1230 cm^{-1}), and linear and bidentate nitrates (bands at 1480 and 1510 cm^{-1}) with increasing temperature, without any other species formation. At 773 K, only a small amount of residual nitrite species are evident, 1300 cm^{-1}, again similar as for NH_3–TPSR (Fig. 9a). However, with increasing ammonia concentration, 333 ppm (Fig. 11b) and 1000 ppm (Fig. 11c), the surface species reduction was faster and more nitrite/nitrate surface species were reduced between 423 and 523 K. The amount of residual species were similar for all TPSR experiments, regardless of ammonia concentration.

To explain the reactivity of preformed nitrates/nitrites in NO + NH_3, it is necessary to take into account reactions (4) and (5) as well as the reactions between nitrates/nitrites and ammonia according to equations (10) and (11):

$$3Ba(NO_3)_2 + 10NH_3 \rightarrow 8N_2 + 15H_2O + 3BaO \quad (10)$$

$$Ba(NO_2)_2 + 2NH_3 \rightarrow 2N_2 + 3H_2O + BaO \quad (11)$$

During TPSR experiment type II with low ammonia concentration (Fig. 10), it was observed that NH_3 was completely consumed, and decomposition of unreacted nitrites occurred at temperatures higher than 623 K. N_2 and N_2O production was observed, which most likely took place according to the stoichiometry of reactions (4) and (5). At low temperatures, below 438 K, reaction (10) occurs to a very small extent, if at all, taking into account the amount of NO and NO_2 from nitrate decomposition, with the decomposition peak maximum at ca. 723 K. Also, with NO present, nitrites/nitrates decomposition is shifted at higher temperature by 20 K, similar to the data shown in Fig. 6 and discussed above. There was no nitrites nor nitrates (Fig. 11, DRIFTS) decomposition up to 438 K. Therefore, presumably up to this temperature only NO and NH_3, which are co-fed to the reactor, participated in reaction (4) and (5) on the Pt sites, forming N_2 and N_2O. At temperatures higher than 473 K, observed nitrates to nitrites reduction, and nitrite decomposition (Fig. 11, DRIFTS), suggests that previously stored N-species also participate in N_2 and N_2O formation.

With a stoichiometric NO to NH_3 concentration (500 ppm NO + 333 ppm NH_3, Fig. 10), the reduction of some nitrites/nitrates occurs at the beginning of the TPSR experiment. Nitrite/itrate reduction takes place in the 448–623 K range; however only ca.15% of all nitrites/nitrates stored are reduced. Above the temperature of nitrites/nitrate stability (623 K), again decomposition of stored nitrites/nitrates can be observed.

Total NO consumption and nitrites/nitrate reduction was obtained when using 1000 ppm of NH_3 (Fig. 10). When NH_3 is not limiting, reaction (5) is almost negligible, reactions (4) and (10) are fast and take place together in the 448–623 K range. Above 623 K no nitrate decomposition peak was observed, indicating that the reduction of stored nitrites/nitrates is complete (the amount of residual nitrites/nitrates is below 0.5%, if any). According to the N-balance and calculations with different ammonia concentrations (Fig. 12), in the later stage of TPSR type II for these experiment conditions, up to 448 K most likely only the co-fed NO and NH_3 react together via reaction (4), and above 448 K the reaction with preformed N-species (nitrites/nitrates) participate towards N_2 and N_2O formation via reactions (10) and (11).

Taking into account the results presented above, it can be assumed that when the reductant is limiting, then the reaction between gas-phase NO and ammonia over the cagtalyst is faster and/or competitive, than the reduction of surface nitrites/ nitrates.

In comparing TPSR type II experiment data (Fig. 10, 166, 333 and 1000 ppm NH_3), with preformed nitrites/nitrates, and type I experiment (Fig. 3) some changes in the NO_2 profile can be observed, and suggest that reaction (9) occurs under the investigated conditions. It can be speculated that during (NO + NH_3)-TPSR reaction with preformed nitrates/nitrites, the reaction between gas-phase NO with NH_3 over the catalyst takes place at the expense of nitrate/nitrite reduction. The decomposition of ammonia via reaction (9) was not observed.

The obtained data reveal that N_2O formation starts at a temperature as low as 373 K and when the ammonia concentration is low, N_2O is produced during all TPSR type II experiments, Fig. 13. Comparing the N_2O profiles of TPSR with and without preformed nitrites/nitrates (Fig. 13 vs 5), an increase in N_2O production is observed with 333 ppm of ammonia (Fig. 13a, b). According to the stoichiometry of reactions (4), (5) and (10), the data suggest that reaction (5) is carried out at the expense of reaction (4) due to the (N-species + NO)/NH_3 ratio and involvement of NH_3 in partial reduction of nitrites/nitrates via reaction (10). Figure 12 shows product mol g^{-1} distributions as a function of ammonia concentration during all TPSR type II experiment, according to reactions (4), (5) and (10). The amount of N_2O produced when NH_3 is in abundance (1000 ppm of NH_3),

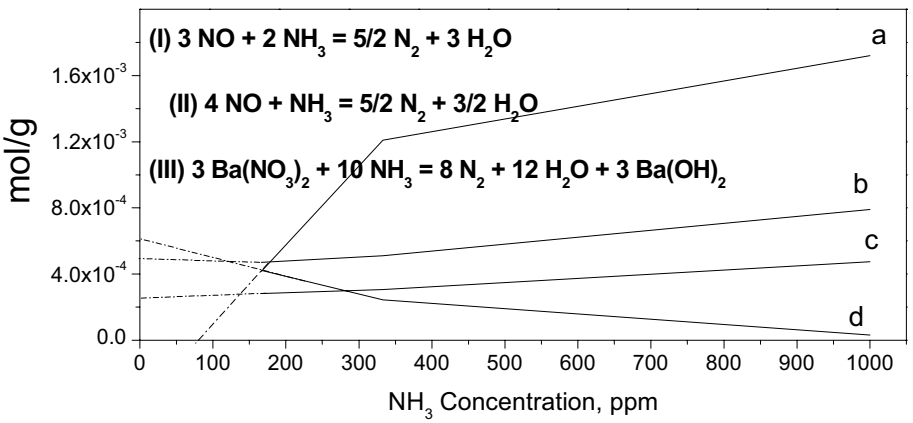

Fig. 12 Product mol g^{-1} distribution as a function of ammonia concentration during TPSR type II experiment: **a** NH_3 consumed with reaction (I) and (II), **b** NH_3 left after reaction (I) and (II), **c** NO_3^- consumed by NH_3 left via reaction (III) and **d** N_2O produced during all experiment

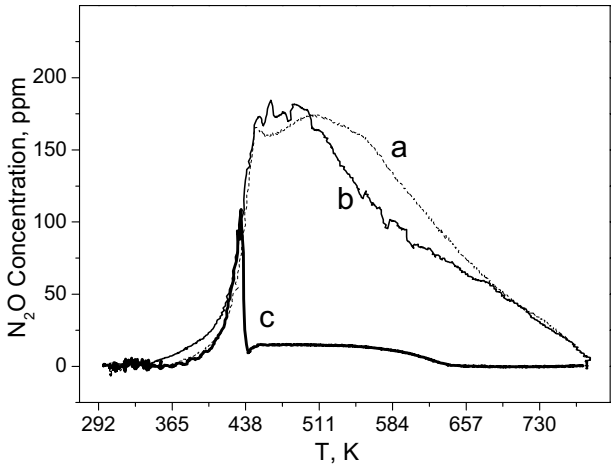

Fig. 13 N_2O production during TPSR type II experiment upon admission of 500 ppm of NO and **a** 166 ppm, **b** 333 ppm and **c** 1000 ppm of NH_3

is roughly constant for both experiments with and without nitrites/nitrates present and is ca. 4×10^{-5} mol/g_{cat}. For all TPSR experiments, a maximum in N_2O production occurs at 448 K.

When taking into account the set of data when 333 ppm of NH_3 was added, i.e. $(NO + NH_3)$-TPSR without preformed nitrites/nitrates, Fig. 5, $(NO + NH_3)$-TPSR with preformed nitrites/nitrates, Fig. 10, and NH_3-TPSR with preformed nitrites/nitrates, Fig. 8, it can be concluded that first the consumption of the NO from the gas phase occurs and later reduction of surface nitrites/nitrates with ammonia. As was found previously, Pt must be involved in the reaction, because the reduction of stored nitrates/nitrites by NH_3 is not effective over Pt-free samples [54, 60]. Moreover, this current study shows that when ammonia is a limiting agent, nitrates/nitrites remain on the catalyst surface unreacted, and at temperatures higher than 623 K decompose. Therefore, this suggests that the reaction between NO and NH_3 on the catalyst is faster/preferential than the reaction between NH_3 and the nitrites/nitrates. Also, most likely weakly adsorbed N-species will react more easily with ammonia than for example bulk nitrates. It has been suggested that nitrates adsorbed on Ba sites in the vicinity of Pt are more easily reduced than N-species adsorbed on Ba sites situated farther away from Pt [61–63].

The calculated conversions and selectivities show that when NH_3 is not limiting, the NO conversion reaches its maximum at ca. 448 K. At the same temperature, the NH_3 conversion reaches 100% and when NH_3 is in abundance, the extra ammonia stays unreacted. In general, for all performed experiments, N_2O was the dominant product at low temperature, when NO and NH_3 conversions are low. At higher temperature, with increasing NO and NH_3 conversions, an increase in reaction (5) prevails and selectivity to N_2 increases. Moreover, the selectivities towards N_2 and N_2O depend on ammonia concentration, which was also proposed previously [61–63]. N_2 is the main product for higher than stoichometric NH_3-to-NO concentrations, while for low NH_3 concentrations, N_2O production is significant.

4 Conclusions

N_2O formation was studied over Pt–Ba/γ–Al_2O_3. The results show:

- N_2O is the dominant product at low temperature, and when NH_3 concentrations are substoichiometric. At higher temperature, with increasing NO and NH_3 conversions, N_2 selectivity increases.
- In characterizing the slopes of the N_2O and N_2 production rates, up to 423 K, it is apparent that the reaction rates are similar. Moreover, the amount of N_2O and N_2 produced up to 423 K indicate that the rates of reaction most likely are not controlled by NH_3 concentration.
- In experiments with nitrites/nitrates on the surface, roughly similar amounts of N_2O are formed, indicating it is gas-phase NO_X leading to N_2O byproduct selectivity.
- In comparing the results from the samples with nitrites/nitrates on the surface to those without, it is apparent that NH_3 first reacts with NO from the gas phase and then nitrites/nitrates.
- The reduction of nitrites/nitrates is complete only for high NH_3/NO ratios, and when NH_3 is the limiting reactant relative to gas-phase NO_x, nitrites/nitrates remain on the catalyst surface unreacted, and at temperatures higher than 623 K decompose giving NO_2 and O_2.

Acknowledgements The present research was financially supported by the Foundation for Polish Science co-financed by the European Regional Development Fund under the Smart Growth Operational Programme PO IR (Project No. REINTEGRATION/2016-1/5). MCR, ML and LA gratefully acknowledge financial support from the Ministry of Education, CTQ2013-47853R.

References

1. Chena Z, Wanga X, Wanga Y, Wanga R (2015) J Mol Catal A 396:8–14

2. Malamis SA, Li M, Epling WS, Harold MP (2018) Appl Catal B 237:588–602
3. Wang P, Yi J, Gu W, Luo P, Lei L (2017) Chem Eng J 325:700–707
4. Xie W, Yu Y, Xie HH (2018) J Environ Sci. https://doi.org/10.1016/j.jes.2018.1006.1013
5. Forzatti P, Lietti L (2010) Catal Today 155:131–139
6. Xu L, McCabe RW (2012) Catal Today 184:83–94
7. You R, Meng M, Zhang J, Zheng L, Hu T, Li X (2018) Catal Today. https://doi.org/10.1016/j.cattod.2018.1003.1022
8. Jabłońska M, Palkovits R (2016) Appl Catal B 181:332–351
9. Mihai O, Widyastuti CR, Andonova S, Kamasamudram K, Li J, Joshi SY, Currier NW, Yezerets A, Olsson L (2014) J Catal 311:170–181
10. Alcalde-Santiago V, Davó-Quiñonero A, Such-Basáñez I, Lozano-Castelló D, Bueno-López A (2018) Appl Catal B 220:524–532
11. Valle SD, Marie O, Nguyen HP (2018) Appl Catal B 223:116–124
12. Anderson JA, Liu Z, Garcia MF (2006) Catal Today 113:25
13. Malpartida I, Larrubia MA, Alemany LJ, Finocchio E, Busca G (2008) Appl Catal B 80:214
14. Cortés-Reyes M, Herrera MC, Pieta IS, Larrubia MA, Alemany LJ (2016) Appl Catal A 523:193–199
15. Pereda-Ayo B, Torre UDL, González-Marcos M, González-Velasco JR (2015) Catal Today 241:133–142
16. Pieta IS, García-Diéguez M, Larrubia MA, Alemany LJ, Epling WS (2013) Catal Today 207:200–211
17. Onrubia JA, Pereda-Ayo B, De-La-Torre U, González-Velasco JR (2017) Appl Catal B 213:198–210
18. Castoldi L, Matarrese R, Morandi S, Righini L, Lietti L (2018) Appl Catal B 224:249–263
19. Epling WS, Campbell LE, Yezerets A, Currier NW, Parks JE (2004) Catal Rev 46:163
20. Pieta IS, García-Diéguez M, Herrera MC, Larrubia MA, Alemany LJ (2010) J Catal 270:256
21. Shimizu K, Saito Y, Nobukawa T, Miyoshi N, Satsuma A (2008) Catal Today 139:24–28
22. Mendes AN, Zholobenko VL, Thibault-Starzyk F, Costa PD, Henriques C (2016) Appl Catal B 195:121–131
23. Ström L, Carlsson P, Skoglundh M, Härelind H (2016) Appl Catal B 181:403–412
24. Zheng Y, Harold MP, Luss D (2016) Catal Today 264:44–54
25. AL-Harbi M, Radtke D, Epling WS (2010) Appl Catal B 96:524–532
26. Beale AM, Gao F, Lezcano-Gonzalez I, Peden CHF, Szanyi J (2015) Chem Soc Rev 44:7371
27. Can F, Courtois X, Royer S, Blanchard G, Rousseau S, Duprez D (2012) Catal Today 197:144–154
28. Lindholm A, Sjövall H, Olsson L (2010) Appl Catal B 98:112–121
29. Elizundia U, Duraiswami D, Pereda-Ayo B, López-Fonseca R, González-Velasco JR (2011) Catal Today 176:324–327
30. Kubiak L, Righini L, Castoldi L, Matarrese R, Forzatti P, Lietti L, Daturi M (2016) Top Catal 59:976–981
31. Masdrag L, Courtois X, Can F, Royer S, Rohart E, Blanchard G, Marecot P, Duprez D (2012) Catal Today 189:70–76
32. Zhu J, Shena M, Wang J, Wang X, Wang J (2017) Catal Today 297:92–103
33. Castoldi L, Matarrese R, Liu C, Morandi S, Lietti L (2018) Top Catal. https://doi.org/10.1007/s11244-018-1022-2
34. Pieta IS, Epling WS, García-Diéguez M, Luo JY, Larrubia MA, Herrera MC, Alemany LJ (2011) Catal Today 175:55
35. Kustov AL, Makkee M (2009) Appl Catal B 88:263
36. Sedlmar C, Seshan K, Jentys A, Lercher JA (2003) J Catal 214:308
37. Toops T, Smith DB, Partridge WP (2005) Appl Catal B 58:245
38. Liu Z, Anderson JA (2004) J Catal 224:18
39. Hadjiivanov KI (2000) Catal Rev Sci Eng 42:71
40. Kromer BR, Cao L, Cumaranatunge L, Mulla SS, Ratts JL, Yezerets A, Currier NW, Ribeiro FH, Delgass WN, Caruthers JM (2008) Catal Today 136:93–103
41. Macleod N, Lambert RM (2003) Appl Catal B 46:483
42. Mosqueda-Jimenez BI, Jentys A, Sehshan K, Lercher JA (2003) Appl Catal B 46:189
43. Broqvist P, Gronbeck H, Fridell E (2004) J Phys Chem B 108:3523
44. Fridell E, Skoglundh M, Westerberg B, Johansson S, Smedler G (1999) J Catal 183:196
45. Ji Y, Toops T, Pihl JA, Crocker M (2009) Appl Catal B 91:329
46. Epling WS, Peden CHF, Szanyi J (2008) J Phys Chem 112:10952
47. Finocchio E, Busca G (2001) Catal Today 70:213
48. Lesage T, Saussey J, Malo S, Hervieu M, Hedouin C, Blanchard G, Daturi M (2007) Appl Catal B 72:166
49. Diesel Exhaust Particulates (2000) Substance profiles, report on carcinogens, 11th edn. U.S. Department of Health and Human Services, Washington, DC
50. Castoldi L, Lietti L, Nova I, Matarrese R, Forzatti P, Vindigni F, Morandi T, Prinetto F, Ghiotti G (2010) Chem Eng J 161:416
51. Szailer T, Kwak JH, Kim DH, Hanson JC, Peden CHF, Szanyi J (2006) J Catal 239:51
52. Konsolakis M, Yentekakis I (2001) J Catal 198:142
53. Konsolakis M, Yentekakis I (2001) Appl Catal B 29:103
54. Castoldi L, Nova I, Lietti L, Tronconi E, Forzatti P (2007) Top Catal 42–43:189
55. Cumaranatunge L, Mulla SS, Yezerets A, Currier NW, Delgass WN, Ribeiro FH (2007) J Catal 246:29
56. Kouakou A, Dhainaut F, Granger P, Fresnet F, Louis-Rose I (2009) Top Catal 52:1734
57. Burch R (2004) Catal Rev Sci Eng 46:271
58. Burch R, Breen JP, Meunier FC (2002) Appl Catal B 39:283
59. James D, Fourre E, Ishii M, Bowker M (2003) Appl Catal B 45:147
60. Forzatti P, Lietti L, Nova I, Tronconi E (2010) Catal Today 151:202
61. Nova I, Castoldi L, Lietti L, Tronconi E, Forzatti P (2007) Top Catal 42:21
62. Nova I, Lietti L, Forzatti P (2008) Catal Today 136:128
63. Nova I, Lietti L, Forzatti P, Frola F, Prinetto F, Ghiotti G (2009) Top Catal 52:1757